Monthly Notices of the ROYAL ASTRONOMICAL SOCIETY

MNRAS **503,** 4092–4104 (2021) doi:10.1093/mnras/stab701
Advance Access publication 2021 March 10

Revisiting the *Kepler* field with *TESS*: Improved ephemerides using *TESS* 2 min data

Matthew P. Battley [1,2]★ Michelle Kunimoto,[3] David J. Armstrong [1,2] and Don Pollacco[1,2]

[1]*Department of Physics, University of Warwick, Gibbet Hill Road, Coventry CV4 7AL, UK*
[2]*Centre for Exoplanets and Habitability, University of Warwick, Gibbet Hill Road, Coventry CV4 7AL, UK*
[3]*Kavli Institute for Astrophysics and Space Research, Massachusetts Institute of Technology, Cambridge, MA 02139, USA*

Accepted 2021 March 2. Received 2021 February 24; in original form 2021 January 8

ABSTRACT

Up to date planet ephemerides are becoming increasingly important as exoplanet science moves from detecting exoplanets to characterizing their architectures and atmospheres in depth. In this work, ephemerides are updated for 22 *Kepler* planets and 4 *Kepler* planet candidates, constituting all *Kepler* planets and candidates with sufficient signal to noise in the *TESS* 2 min data set. A purely photometric method is utilized here to allow ephemeris updates for planets even when they do not posses significant radial velocity data. The obtained ephemerides are of very high precision and at least seven years 'fresher' than archival ephemerides. In particular, significantly reduced period uncertainties for Kepler-411d, Kepler-538b, and the candidates K00075.01/K00076.01 are reported. O–C diagrams were generated for all objects, with the most interesting ones discussed here. Updated TTV fits of five known multiplanet systems with significant TTVs were also attempted (Kepler-18, Kepler-25, Kepler-51, Kepler-89, and Kepler-396), however these suffered from the comparative scarcity and dimness of these systems in *TESS*. Despite these difficulties, *TESS* has once again shown itself to be an incredibly powerful follow-up instrument as well as a planet-finder in its own right. Extension of the methods used in this paper to the 30 min-cadence *TESS* data and *TESS* extended mission has the potential to yield updated ephemerides of hundreds more systems in the future.

Key words: ephemerides – time – planets and satellites: fundamental parameters – planets and satellites: general.

1 INTRODUCTION

Maintenance of planet ephemerides is crucial to further characterization of known planets. This is especially true for follow-up with high-profile observatories such as the upcoming *James Webb Space Telescope* (*JWST*; Gardner et al. 2006), where timing uncertainties of less than 30 min are desirable (Dragomir et al. 2020). Furthermore, ensuring that ephemerides of known planets and planet candidates remain fresh secures the legacy of large-scale planet-finding missions such as those performed by the *Kepler* satellite (Borucki et al. 2010) and the *Transiting Exoplanet Survey Satellite* (*TESS*; Ricker et al. 2014).

The *Kepler* satellite dramatically changed the field of exoplanet science, discovering almost 3000 validated exoplanets and thousands more planet candidates over the course of its main mission and following *K2* mission (Howell et al. 2014). However, the original *Kepler* mission finished 2013 May 11 after the failure of two of the satellite's reaction wheels,[1] meaning that it has now been over seven years since most of these planets have been observed. This observational gap, coupled with uncertainties in the periods and epochs of the *Kepler* transits, has led to many of the planet/candidate ephemerides becoming imprecise or 'stale'.

A number of different surveys have attempted to solve this problem, both for *Kepler* and *K2* planets (e.g. Livingston et al. 2019; Edwards et al. 2020; Ikwut-Ukwa et al. 2020), however the sheer number of planets and candidates discovered by the satellite makes this a significant challenge. Promising follow-up solutions include re-observing the entire *Kepler* field or using large-scale citizen-science approaches (e.g. Kokori et al. 2020; Zellem et al. 2020). The launch of *TESS* in 2018 provides a new opportunity to address this challenge. Having already completed its 2-yr primary mission, *TESS* has surveyed ∼75 per cent of the night sky. During this mission, *TESS* returned to the original *Kepler* field, providing new data for the *Kepler* field in Sector 14 (and to a lesser extent, Sectors 15 and 26) of its observations.

Ikwut-Ukwa et al. (2020) have previously demonstrated the significant impact re-observing data from the *Kepler* satellite with *TESS* can have, completing full ephemeris and wider system parameter updates for K2-114, K2-167, K2-237, and K2-261 by utilizing a combined photometric (*TESS* and *Kepler* data) and spectroscopic (using archival radial velocities) measurements. In the case of K2-114 these new measurements were shown to reduce the uncertainty in the planet's period by a factor of 66 (Ikwut-Ukwa et al. 2020) compared to its discovery period. This promising result heralds the way for a wider treatment of the entire *TESS/Kepler* crossover sample in order to have ephemerides ready for the launch of *JWST*.

Furthermore, Christ, Montet & Fabrycky (2018) point out that re-observing the *Kepler* field with *TESS* provides a host of additional

★ E-mail: Matthew.Battley@warwick.ac.uk
[1]https://archive.stsci.edu/missions/kepler/docs/drn/release_notes25/KSCI-19065-002DRN25.pdf

benefits, providing a window into long-term trends such as tidal decay of Hot Jupiters. In particular, Christ et al. (2018) suggest that the Hot Jupiters Kepler-2b/HAT-P-7 and KOI-13b will be particularly interesting objects to follow up with *TESS* data. They also suggest that *TESS* may be very powerful for investigating longer term transit timing variations. These thoughts are echoed by the modelling of Goldberg et al. (2018) where they conclude that mass uncertainties could be improved for 6-14 planets with the new *TESS* 2 min data, depending on the eventual measurement uncertainties.

While the combined photometric/spectroscopic approach of Ikwut-Ukwa et al. (2020) allowed for new global models of the systems to be created, many of the lower mass Kepler planets and candidates do not currently possess significant radial-velocity data. This motivates the construction of a homogeneous method of updating new ephemerides based on *TESS/Kepler* photometry alone. Such a method is presented in this paper, along with the updated ephemerides for every *Kepler* planet and candidate which was reasonably re-observed in the *TESS* 2 min data.

Section 2 describes the *Kepler* and *TESS* observations used in this analysis. This is followed by the methods used to obtain the individual transit times and updated ephemerides in Section 3 before the results are presented in Section 4. Implications of these results are discussed further in Section 5 before a summary of the work carried out. Note that a wider list of all *Kepler* planetary systems which received *TESS* short-cadence data is included in the appendix, including reasons why excluded systems were removed from the analysis.

2 OBSERVATIONS

2.1 *Kepler*

Kepler's primary mission ran for approximately four years, or 17 'quarters', from first light on 2009 May 2 until the loss of the satellite's second reaction wheel in 2013 May. Observing the same rich patch of sky in the vicinity of the Cygnus and Lyra constellations for its entire primary mission, the *Kepler* satellite yielded an unprecedented volume of high quality, long-duration photometry, and was the first telescope capable of finding Earth-sized planets around Sun-like stars in year-long orbits (Borucki et al. 2010). The majority of the targets in the *Kepler* mission's primary field were observed in *Kepler's* 29.4 min (30 min) long-cadence mode, however approximately 512 objects per quarter received 1 min short-cadence light-curves covering a month in time (Thompson et al. 2016).

In this work, *Kepler* long-cadence PDCSAP light curves were retrieved from the public Mikulski Archive for Space Telescopes (MAST)[2] using the *Lightkurve* PYTHON package (Lightkurve Collaboration 2018). These light curves were prepared by the standard *Kepler* science processing pipeline (Jenkins et al. 2010), which involves pixel-level calibration, smear and background removal, optimal aperture selection and modelling of systematic errors introduced by the spacecraft. Due to the stellar variability of most sources over the long *Kepler* observation timeline, an additional detrending step was necessary before planetary transits could be used to update ephemerides. This was achieved by applying a simple 24 h window LOWESS filter (Cleveland 1979; Battley, Pollacco & Armstrong 2020) to the out-of-transit light curve, except in the cases such as Kepler-9 (Holman et al. 2010), where shorter 12–15 h windows were required to handle the shorter period activity cycles. In order to preserve the form of each individual transit, the transit epochs were masked from the light curves during this detrending step and replaced with linear interpolations until the detrending was complete.

[2]https://mast.stsci.edu/portal/Mashup/Clients/Mast/Portal.html

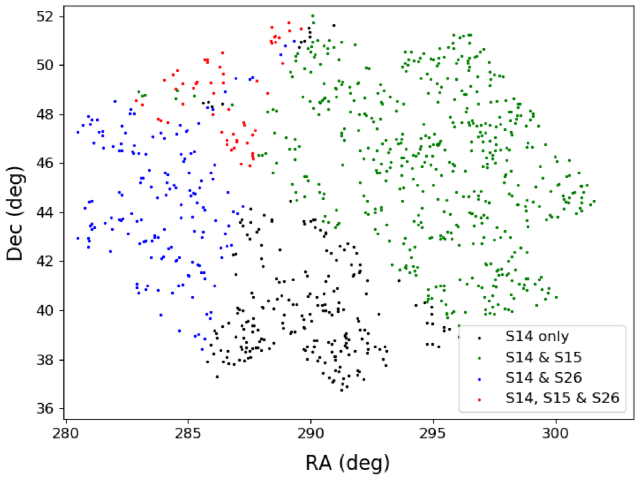

Figure 1. Overview of *Kepler* stars reobserved by *TESS* with 2 min cadence. Individual stars are colour-coded according to which *TESS* sectors they were observed in: Black: Sector 14 only; Green: Sectors 14 and 15; Blue: Sectors 14 and 26; Red: Sectors 14, 15 and 26.

2.2 *TESS*

TESS re-observed the *Kepler* field in the second year of its primary mission. The majority of the Kepler field was observed in Sector 14 (between 2019 July 18 and August 15), but due to overlap in adjacent *TESS* observations, some of these stars were also re-observed in Sectors 15 (2019 August 15–September 11) and 26 (2020 June 8–July 4). However, although the entire *Kepler* field was re-observed in Sector 14 of the *TESS* primary mission, only 962 Kepler stars were pre-selected to receive 2 min data in *TESS*'s primary mission. These stars are plotted in Fig. 1, colour-coded by which sectors they were re-observed in.

All *TESS* light curves used in this work were generated by NASA's Science Processing Operations Centre (SPOC) and, similar to the *Kepler* data, accessed using the *Lightkurve* PYTHON package (Lightkurve Collaboration 2018). These data were extracted from the raw images using the standard SPOC pipeline (Jenkins et al. 2016), which includes pixel-level decorrelation, centroiding, and aperture optimization. For all light curves the PDCSAP flux data were analysed, which had previously had systematic errors such as times of poor pointing or excessive scattered light removed (Jenkins et al. 2016). Similar to the *Kepler* data, after extraction via the Lightkurve package, long-term stellar variability outside the transit was removed from the *TESS* 2 min light curves using a 24 h window LOWESS filter.

2.3 *Photometry comparison*

The *Kepler* and *TESS* missions were designed with two very different survey strategies in mind, and hence differ in their photometric performance. While the *Kepler* mission focused on a relatively small (100 deg^2, or 0.25 per cent of the sky) Northern hemisphere section of the sky near the Cygnus, Lyra, and Draco constellations (Borucki et al. 2010), the *TESS* primary mission focused on maximizing the amount of sky viewed, achieving almost 75 per cent coverage of the

sky[3] in its two year primary mission, updated from the originally planned 85 per cent due to issues with scattered light (Ricker et al. 2014). To achieve this coverage with *TESS*, a slight sacrifice in sensitivity was required, with combined differential photometric precision (CDPP) dropping from an average of 30 ppm for the *Kepler* mission (Gilliland et al. 2011) to approximately 100 ppm[4] for Sector 14 of the *TESS* mission. This reduced sensitivity comes from a variety of sources, but most importantly the reduced effective lens size in *TESS* due to reducing from a single large mirror (effective lens diameter of 95 cm) on the *Kepler* satellite to smaller 10.5 cm lens-based telescopes in *TESS*. This reduction in effective lens diameter results in the lower resolution of the *TESS* instruments (21 arcsec per pixel instead of Kepler's 4 arcsec per pixel) and yields increased blending from nearby stars compared to the *Kepler* satellite. The combination of these effects, coupled with the shorter observational time-scale in *TESS* (27 d to 1 yr in *TESS*; 4 yr in *Kepler*), means that *TESS* is less sensitive to small planets than *Kepler* was, with Christ et al. (2018) predicting that only 277 *Kepler* planets have a >50 per cent likelihood of being recovered by *TESS* to a 3σ level in the wider-extent 30 min cadence data.

This issue is well illustrated in Fig. 2, showing the comparison between *Kepler* and *TESS* data for a large Jupiter-sized planet (HAT-P-7 b; Pál et al. 2008) and a small Super-Earth sized planet (Kepler-21b; Howell et al. 2012). While the planetary signal for both systems is clear in the *Kepler* data, the smaller planet is entirely indiscernible in the 2 min *TESS* light curve. This perhaps helps to explain why only seven known *Kepler* planets reobserved with *TESS* 2 min cadence were identified as *TESS* Objects of Interest (TOIs).[5]

For the purpose of this study, we focus on all *Kepler* confirmed planets and candidates with transits visible in the *TESS* 2 min data, including many that were missed as *TESS* TOIs.

2.4 Overall target selection

In order to find all *Kepler* planets and candidates which received 2 min *TESS* data, the 962 *Kepler* stars with short-cadence data were cross-matched with all transiting planets and *Kepler* planet candidates from the NASA Exoplanet Archive.[6] This revealed a population of 49 *Kepler* planetary host stars (harbouring 93 transiting planets) and 28 planet candidate systems which were re-observed by *TESS* in its short-cadence mode. However, due to the comparatively short (28 d) *TESS* observation window compared to some long-period *Kepler* planets, the expected transit times were missed for 19 planets and 8 planet candidates, making them unusable for ephemeris updates. Note that the planetary system of Kepler-34 (TIC 164457525) was also removed, as its planet is not expected to transit again until 2066 November 18 due to its complex circumbinary orbit (Welsh et al. 2015; Martin 2017).

The *TESS* 2 min light curves for the remaining 73 transiting planets and 20 planet candidates were searched for new transits both by eye and systematically with a box-least-squares search (Kovács, Zucker & Mazeh 2002; Hartman & Bakos 2016), as implemented as the `BoxLeastSquares` function in the `astropy` PYTHON package (Astropy Collaboration 2013, 2018). Because of the reduced sensitivity of the *TESS* instrument, many of the smallest *Kepler* planets were indiscernible from noise in the *TESS* data alone, so these systems were also cut from the analysis. Overall there remained 22 planets (in 18 planetary systems) and 4 planet candidates where the ephemerides could be reasonably improved using the *TESS* 2 min data. It is worth noting however that for many of these only a single transit was observed. Table 1 gives an overview of the final systems which have been updated in this study, while a system by system summary of this target selection is included for each planet host in Table A1.

[3]https://www.nasa.gov/feature/goddard2020/nasa-s-planet-hunter-completes-its-primary-mission

[4]https://archive.stsci.edu/missions/tess/doc/tess_drn/tess_sector_14_drn19_v02.pdf

[5]https://exofop.ipac.caltech.edu/tess/view_toi.php

[6]https:exoplanetarchive.ipac.caltech.edu [Accessed 12 August 2020]

3 METHODS

3.1 Assembling archival system parameters

As a starting point for the models, planetary and stellar parameters were retrieved from the NASA Exoplanet Archive for all objects. In cases where the data highlighted on the exoplanet archive was out of date, these parameters were updated to reflect the most recent literature. In order to collect the most recent radii information, the entire sample was cross-matched with Berger et al. (2018)'s revised radii of *Kepler* stars and planets based on *Gaia* DR2 data (Gaia Collaboration 2018; Lindegren et al. 2018). This list was then cross-matched with the updated linear ephemerides found by Gajdos, Vanko & Parimucha (2019), who used the entire length of *Kepler* data (Q1-17) to update ephemerides for 1977 exoplanets. As a first check for significant transit timing variations, the TTV flag was checked on the Exoplanet Archive, and all systems cross-matched with TTV data from surveys completed by Holczer et al. (2016) and Gajdos et al. (2019).

Similar to the *Kepler* planets, original data for the *Kepler* planet candidates was collected from the *Kepler* Objects of Interest (KOI) list on the Exoplanet Archive, taking care to disregard any KOIs previously downgraded to false positives. These data were then cross-matched with data from the most recent TESS Input Catalogue (TICv8; Stassun et al. 2019) and Berger et al. (2018)'s revised radii of *Kepler* stars and planets to obtain up-to-date information for the stellar hosts.

3.2 Ephemeris updates and construction of O–C diagrams

The methods used to determine individual transit times and update linear ephemerides are based on those used by Gajdos et al. (2019) and Holczer et al. (2016) to analyse the full Kepler Q1-17 data. As a first step, transit epochs for planets/candidates other than the one being currently analysed were masked from the light curve. In some cases with large TTVs (such as Kepler-396b; Xie 2014), the masking window was widened slightly to catch all of the transits. Because of the differing dilution characteristics and data cadence of the *Kepler* and *TESS* instruments, the *Kepler* transits were found first and then the results from this analysis were used to inform the initial *TESS* model.

To achieve consistent times for the two satellites, the time data for both data sets was converted to Barycentric Julian Date using the following conversions:

(i) $Kepler_{\mathrm{BJD}} = \mathrm{KBJD} + 2454833\,\mathrm{d}$
(ii) $TESS_{\mathrm{BJD}} = \mathrm{BTJD} + 2457000\,\mathrm{d}$

For the first step in the *Kepler* analysis, a Mandel & Agol (2002) transit model was constructed for the object of interest using Kreidberg (2015)'s `batman` software, based off the archival parameters assembled in Section 3.1. These models were used to

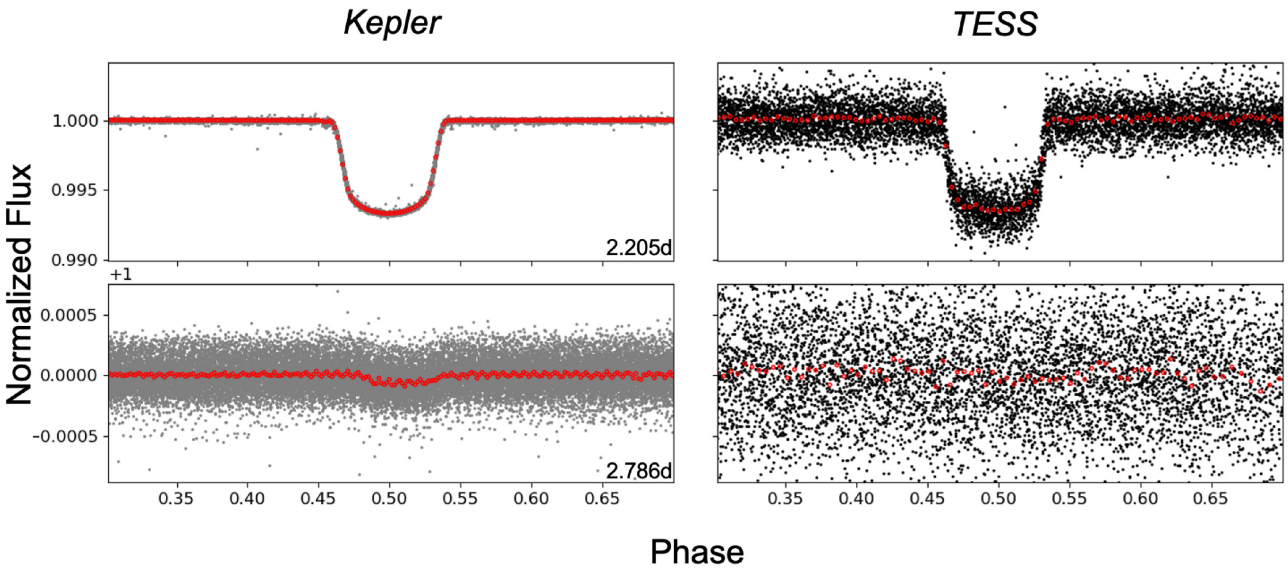

Figure 2. Photometric data comparison between *Kepler* (left-hand panel) and *TESS* (right-hand panel). Top: HAT-P-7 b/Kepler-2b, a 1.51 $M_{\rm Jup}$ Hot Jupiter is clearly recovered by both *Kepler* and *TESS*. Bottom: Kepler-21b, a 1.6$M_{\oplus}$ super-Earth is clear in the folded *Kepler* data but lost in scatter in the *TESS* data.

Table 1. Overview of final *Kepler* planetary and candidate systems for which ephemerides were updated in this study. A TTV flag of '1' denotes any systems where unusual/non-linear behaviour was observed in the O–C diagrams constructed in this work.

	Planets		
System name	Planets updated	TTV flag	Discovery paper
Kepler-2/HAT-P-7	b	1	Pál et al. (2008)
Kepler-10	c	1	Fressin et al. (2011)
Kepler-13/KOI-13	b	0	Borucki et al. (2011)
Kepler-14	b	0	Buchhave et al. (2011)
Kepler-18	d	1	Cochran et al. (2011)
Kepler-25	b, c	1	Steffen et al. (2012)
Kepler-51	b	1	Steffen et al. (2013)
Kepler-51	d	1	Masuda (2014)
Kepler-63	b	0	Sanchis-Ojeda et al. (2013)
Kepler-68	b	0	Gilliland et al. (2013)
Kepler-89/KOI-94	d	1	Weiss et al. (2013)
Kepler-96	b	0	Marcy et al. (2014)
Kepler-289	c	1	Rowe et al. (2014)
Kepler-396	b, c	1	Xie (2014)
Kepler-411	c	1	Morton et al. (2016)
Kepler-411	d	1	Sun et al. (2019)
Kepler-412	b	1	Deleuil et al. (2014)
Kepler-448/KOI-12	b	1	Bourrier et al. (2015)
Kepler-538	b	0	Morton et al. (2016)
Kepler-1517	b	0	Morton et al. (2016)
	Candidates		
System name	Candidates updated	TTV flag	
KIC 7199397	K00075.01	1	
KIC 8554498	K00005.01	0	
KIC 9955262	K00076.01	1	
KIC 9418619	K06068.01	0	

search for the observed transit time by minimizing the chi-squared statistic in a grid of 1 min resolution around the expected transit. This method, similar to that used by Holczer et al. (2016), ensured that the approximate initial transit times could be obtained automatically even

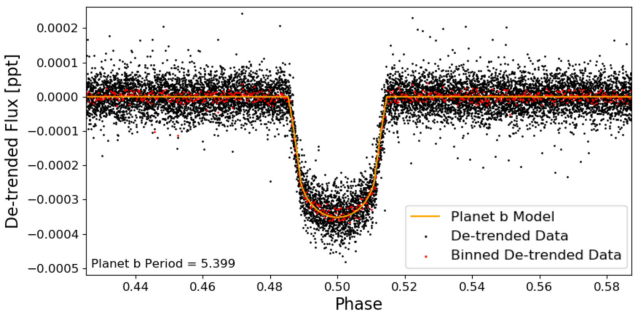

Figure 3. Stacked transit curve for Kepler-68b overplotted with final `batman` model.

when there were significant TTVs present. These 1 min resolution transit times were used to construct a 'stacked' light curve for each planet/candidate by aligning the obtained transit centres, similar to the method used by Gajdoš et al. (2017), Gajdos et al. (2019) (see Fig. 3). This stacked transit was compared to the transit curve obtained simply by folding the *Kepler* data by the known planetary period, with the cleanest transit curve taken forward for further analysis. The dual approach ensured that accurate transit curves could be obtained for targets both with and without transit timing variations. The chosen transit curve was fitted with a new `batman` model using three iterations of the in-built `optimize` routine within `exoplanet` (Foreman-Mackey et al. 2020). Because the individual transit times here are considered more important than the overall system parameters, the planetary radius and inclination were allowed to vary slightly in order to fit the phase-curve most effectively. Note that both parameters were modelled as normal distributions with means equal to value reported in literature (or 90° for systems without published inclinations). The mean value outside each transit was also allowed to vary in case it was skewed by outliers or detrending artefacts. An example of the final transit model can be seen for Kepler-68 b (Gilliland et al. 2013) in Fig. 3.

The generated transit model was used to find precise transit times for individual transits in the *Kepler* data. This was achieved by

cutting out short-duration windows around each expected transit (2 d either side of the transit, unless the planet period was ≤2 d) and finding the best fit of the transit model within that interval. For consistency only the transit time and mean flux were allowed to vary in this step, both of which were set as wide normal distributions centred on the values found from the chi-squared fit. To begin with, three iterations of `exoplanet`'s inbuilt `optimize` routine were used to hone in on the true transit times, before PyMC3 (Salvatier, Wiecki & Fonnesbeck 2016) was used to fit the final planet model to each individual *Kepler* transit. This was achieved using a two-chain Markov Chain Monte Carlo (MCMC) analysis with 1000 tuning steps and 5000 draws for each object. Longer chains were tested briefly, but increasing the length further for these relatively simple fits was not found to change the results significantly. Convergence was assessed using the Gelman–Rubin statistic and a visual examination of the trace. Statistically significant values for the final time and error for each individual transit were then found from the mean and standard deviation of the MCMC trace.

Because of the dearth of *TESS* transits, broadly the same model built from the *Kepler* data was used to find the times of the individual *TESS* transits, however the depth of the transit was adjusted according to the local dilution characteristics of the *TESS* environments. Once again the model was fit to each transit in turn (in a 4-d data interval centred on the expected transit time) using three iterations of `exoplanet`'s `optimize` function and a `pyMC3` MCMC analysis with 10 000 tuning steps and 10 000 draws in order to gain statistically significant values and errors for each mid-transit time.

After the time of each individual *TESS* and *Kepler* transit was determined, the linear ephemeris based on the combined data sets was calculated. An uncertainty-based requirement of $\sigma_{\text{transit}} < 0.2$ h was found to remove the majority of the questionable transits prior to further analysis (typically those which fell in data gaps or were incomplete), however the remainder were viewed by eye to catch any other transits which clearly had been fitted incorrectly. The remaining data points were fit using three iterations of a weighted linear least-squares fit while varying the initial transit time, T_0, and period P. The resulting ephemerides were used to generate an observed–calculated (O–C) plot for each object, providing a visual check for odd behaviour, significant TTV signals or significant outliers. An example O–C plot is shown in Fig. 4 for KOI-13 b. Some of the most interesting O–C diagrams are discussed in the results below (Section 4).

Because of the long data gap between the *Kepler* and *TESS* observation windows, one slight concern was the introduction of cycle count errors, i.e. miscalculating the number of transits between the *Kepler* and *TESS* transits. To check whether this was significant, the archival error in period derived from the *Kepler* data alone was multiplied by the number of missing transit cycles between the final *Kepler* transit and first *TESS* transit. In all cases this was found to result in a value at least two orders of magnitude smaller than a whole transit cycle, hence the ephemerides derived in this work are considered free of cycle count errors.

For any objects which did not display significant TTVs in their O–C diagrams (labelled with '0' in the TTV flag column of Table 1), an additional simultaneous *Kepler/TESS* MCMC fit was carried out on the entire light curve in order to narrow down the precision for these planets/candidates further. This was achieved by fitting the model based on the stacked transit parameters to the entire data set and allowing t0, the mean out-of-transit value and the planetary period to vary. Once again, 1000 tuning steps and 5000 draws were used in this MCMC analysis, using PYMC3 (Salvatier et al. 2016) within `exoplanet` (Foreman-Mackey et al. 2020), following three `optimize` iterations.

3.3 TTV analysis

The updated systems in this work included a number of *Kepler* multiplanet systems known to exhibit significant TTVs, namely Kepler-18, Kepler-25, Kepler-51, Kepler-89, and Kepler-396 (Cochran et al. 2011; Steffen et al. 2012, 2013; Weiss et al. 2013; Masuda 2014; Xie 2014). Most of these systems were independently highlighted as worthwhile systems for further TTV analysis by Goldberg et al. (2018) and/or Jontof-Hutter et al. (2021). In an attempt to update the TTV masses for planets in these systems, additional TTV fitting was carried out. Midtransit times for each planet in a system were simulated using `TTVFast`, a symplectic integrator for computing transit times given a set of planet masses and orbital parameters (Deck et al. 2014). With these simulations, an MCMC analysis explored the parameter space to find the best-fitting masses and orbits describing the observed transit times, both before and after the addition of *TESS* datapoints.

Each transiting planet in a system was fit for mass, μ_i (in units of solar masses), orbital period, P_i, orbital eccentricity, and argument of pericentre (via eccentricity vectors $h_i = \sqrt{e_i}\cos\omega_i$ and $k_i = \sqrt{e_i}\sin\omega_i$), and time of first transit, T_i, where $i = 1, 2, ..., N$ and N is the number of planets. Coplanar orbits were assumed. Guess parameters were estimated using a Levenberg–Marquardt least-squares algorithm, and datapoints more than 4σ from this initial best-fitting solution were marked as outliers and removed from the data. MCMC analysis was then performed using the affine invariant ensemble sampler `emcee` (Foreman-Mackey et al. 2012), with 100 walkers initialized in a tight ball around the guess parameters. Each walker was run for 200 000 steps, and the first 50 000 steps were discarded as burn-in.

Following the procedure of Hadden & Lithwick (2016, 2017), both 'default' and 'highmass' priors were considered, recognizing that TTV fits are often challenged by mass-eccentricity degeneracies. Under the default run, mass was assigned a logarithmic prior

$$p(\mu) \propto \begin{cases} (\mu + \mu_0) & \mu \geq 0, \\ 0 & \text{otherwise} \end{cases} \tag{1}$$

with $\mu_0 = 3 \times 10^{-7}$ to prevent divergence at $\mu \to 0$, while eccentricity was assigned a uniform prior

$$p(h,k) \propto \begin{cases} (h^2+k^2)^{-1/2} & (h^2+k^2)^{1/2} < 0.9, \\ 0 & \text{otherwise} \end{cases} \tag{2}$$

with an upper cutoff at 0.9 to avoid the need for extremely small time-steps in the `TTVFast` integrations. For the high-mass run, mass was assigned a uniform prior

$$p(\mu) \propto \begin{cases} \text{constant}, \mu \geq 0, \\ 0 & \text{otherwise} \end{cases} \tag{3}$$

while eccentricity was assigned a logarithmic prior

$$p(h,k) \propto \begin{cases} (h^2+k^2)^{-1/2}(\sqrt{h^2+k^2}+e_0)^{-1} & (h^2+k^2)^{1/2} < 0.9, \\ 0 & \text{otherwise} \end{cases} \tag{4}$$

with $e_0 = 10^{-3}$ to prevent divergence at $e \to 0$. In both runs, period and initial transit time were assigned uniform priors.

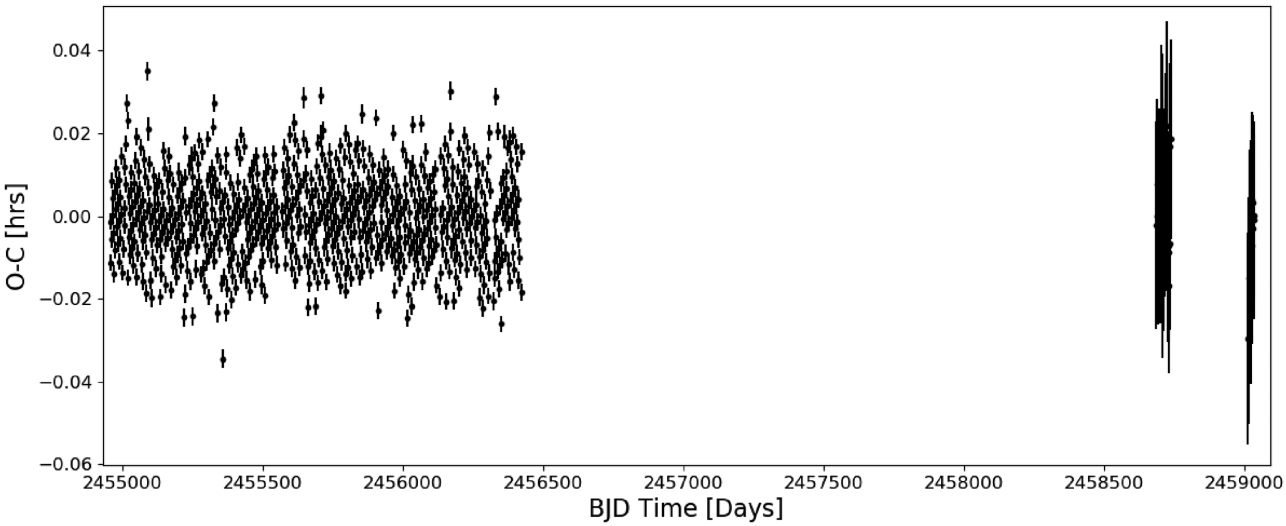

Figure 4. Example O–C plot for Kepler-13/KOI-13b. K0I-13 b received *TESS* 2 min data in Sectors 14, 15, and 26, so represents one of the targets which received the most new data from *TESS*'s primary mission.

4 RESULTS

4.1 Known planets

All ephemerides updated in this study are presented in Table 2, with known planets in the top section of the table and the four planet candidates presented underneath. Here the overall results for the known planets are presented, with a few of the most interesting systems investigated in more depth.

Overall good agreement was found for all updated planet ephemerides when compared to those from the *Kepler* alone. With one exception (Kepler-51d; Masuda 2014), all new periods were within 3σ of their archival values, despite the very precise measurement errors. Any differences between new and archival T_0s can easily be explained by different individual transits being chosen as the zero-point. The difference in period for Kepler-51d is perhaps not surprising given the known transit timing variations of this planet coupled with its long period (130.2 d). Indeed, only nine reasonable transits were captured in the *Kepler* data, and only a single transit in the data from *TESS*'s primary mission. Because of the >8 yr gap between *Kepler* and *TESS* observations and the inclusion of the new *TESS* data increasing the available number of data points by 11 per cent, the new ephemeris found in this study is favoured. The transit timing variations for this planet are plotted in Fig. 5 and explored further in Section 4.3 below.

The overall precision for each ephemeris was found similar to those derived by Gajdos et al. (2019), likely because both their study and this one used the entirety of the *Kepler* data to define the planet ephemerides. The new *TESS* data were thus most useful for improving the precision for planets whose most recent ephemerides came from different sources to Gajdos et al. (2019), namely Kepler-2/HAT-P-7b, Kepler-13b, Kepler-18d, Kepler-289c, Kepler-396b & c, Kepler-411c & d, and Kepler-538b (Pál et al. 2008; Borucki et al. 2011; Cochran et al. 2011; Rowe et al. 2014; Xie 2014; Morton et al. 2016; Sun et al. 2019, see Table 2 for most recent ephemeris references). It should be noted that due to the typically shallower transits recovered in the *TESS* data, the uncertainties in each *TESS* transit are considerably higher than those of each *Kepler* transit, which helps to explain why the new *TESS* data are less constraining than initially expected.

Of the Kepler planets studied in this work, only KOI-13/Kepler-13b (Borucki et al. 2010; Fig. 4) has previously been updated with the newly available *TESS* data. This is presented by to Szabó et al. (2020), who find a period of $1.76358760 \pm 0.00000003$ d, and a T_0 of $2455101.707254 \pm 0.000012$ BJD, in clear agreement with the values obtained in this work (see Table 2). Similar to to Szabó et al. (2020), no evidence of TTVs or tidal decay of this Hot Jupiter was seen in this study. It should be noted that though the eventual ephemeris reported for Kepler-13b in this work was drawn from a simultaneous *TESS/Kepler* fit of the entire light curve, the ephemeris obtained using the initial TTV-focused (transit-by-transit) fit was also in clear agreement, with a value of $T_0 = 2454955.32946735 \pm 0.000006153$ and Period $= 1.76358760059 \pm 0.00000001281$. This system thus provides a useful test-case for the overall methods used in the wider analysis carried out in this work.

One planetary O–C diagram of particular note in this work is that for Kepler-2b/HAT-P-7b, a bright (Gmag $= 10.365$), well-studied Hot Jupiter ($2.0\,R_J$) originally discovered by Pál et al. (2008). This was previously identified as being a prime target for testing orbital decay by Christ et al. (2018). As can be clearly seen in Fig. 6, a slight (2.5 min) offset was found to exist between the original *Kepler* data zero-point and new *TESS* data. While extending the errors of the *TESS* data points to two or three standard deviations would put them in agreement with the general *Kepler* trend, the observed shift is still considered odd given that the excellent timing agreement for similar Hot Jupiter systems such as KOI-13/Kepler-13b and Kepler-412b. In an attempt to solve this discrepancy, additional transits for HAT-P-7b were sought from the Exoplanet Transit Database[7] (Poddaný, Brát & Pejcha 2010), however given the even larger timing uncertainties from the ground based data, no trend was evident. It should be noted though that the original discovery t0 (Pál et al. 2008) also aligns with a slight timing offset of 2.5 min above this *Kepler* zero-point. It is hoped that further data from space telescopes (such as when *TESS* returns to the *Kepler* field in year four of its mission) will help to test whether this shift is real.

Another particularly interesting system updated here is Kepler-411d (Fig. 7). While only one transit was caught in the *TESS*

[7]http://var2.astro.cz/ETD/etd.php?STARNAME=HAT-P-7&PLANET = b

Table 2. Overview of all ephemerides updated in this work. Planet ephemerides are presented first, followed by the four planet candidates. Presented uncertainties are the 1σ uncertainty for each value. n.b.'Ref' refers to the reference each component of the archival ephemerides are drawn from, typically the most recent for each system: 1. Bonomo et al. (2017); 2. Gajdos et al. (2019); 3. Szabó et al. (2020) 4. Holczer et al. (2016); 5. Su et al. (2020); 6. Mayo et al. (2019). All archival information for the four candidates was retrieved from the *q1_q17_dr25_koi* KOI data release (Thompson et al. 2018). A machine-readable copy of this table can be found in the online supplementary material.

		Planets			
Planet name	Archival T_0 (BJD)	Archival period (d)	Ref.	Updated T_0 (BJD)	Updated period (d)
Kepler-2b	2454954.357462 ± 0.000005	2.204737 ± 0.000017	1	2454954.3585572 ± 0.0000063	2.20473539167 ± 0.00000001654
Kepler-10c	2455062.2665100 ± 0.0004297	45.29430079 ± 0.00003051	2	2454971.6772661 ± 0.0006847	45.29426146 ± 0.00003783
Kepler-13b	2455101.707254 ± 0.000012	1.76358760 ± 0.00000003	3	2454953.56595833 ± 0.00003827	1.76358750002 ± 0.00000002147
Kepler-14b	2454971.08821000 ± 0.00006808	6.7901211029 ± 0.0000005613	2	2454957.50815829 ± 0.00008051	6.7901236131 ± 0.0000003985
Kepler-18d	2454961.155156 ± 0.000661	14.85891873 ± 0.00000074	4	2454961.1542075 ± 0.0002423	14.858908757 ± 0.0000004364
Kepler-25b	2455004.7108100 ± 0.0001007	6.2385326915 ± 0.0000007349	2	2454954.7979391 ± 0.0002168	6.2385347882 ± 0.0000001619
Kepler-25c	2455011.52792000 ± 0.00007383	12.720374906 ± 0.000001158	2	2454960.6467450 ± 0.0001144	12.720370495 ± 0.000001703
Kepler-51b	2455714.5917200 ± 0.0001741	45.15530956 ± 0.00001897	2	2454992.10682769 ± 0.0003851	45.15529233 ± 0.00002211
Kepler-51d	2455695.9210000 ± 0.0002442	130.17662541 ± 0.00007274	2	2455045.0339014 ± 0.0004519	130.17784455 ± 0.00008134
Kepler-63b	2455010.84340000 ± 0.00002768	9.4341503479 ± 0.0000003339	2	2454954.23899519 ± 0.00003794	9.4341522797 ± 0.0000004323
Kepler-68b	2455006.85878000 ± 0.00007639	5.3987525913 ± 0.0000005231	2	2454958.2700925 ± 0.0009446	5.398752420 ± 0.000003113
Kepler-89d	2454965.7417600 ± 0.0001014	22.342971172 ± 0.000002603	2	2454965.7413033 ± 0.0001169	22.342982351 ± 0.000002982
Kepler-96b	2455004.02020000 ± 0.00008997	16.238459306 ± 0.000001893	2	2454955.3013031 ± 0.0001767	16.238459945 ± 0.000005665
Kepler-289c	2455069.661672 ± 0.002848	125.86526539 ± 0.00000325	4	2455069.6605154 ± 0.0002487	125.86521071 ± 0.00004151
Kepler-396b	2454995.495267 ± 0.005940	42.99292187 ± 0.00000635	4	2454995.4942951 ± 0.0004076	42.99292140 ± 0.00002072
Kepler-396c	2455015.677038 ± 0.019460	88.51067812 ± 0.00002174	4	2455104.1858280 ± 0.0002890	88.51097554 ± 0.00003917
Kepler-411c	2454968.2224 ± 0.0002	7.834435 ± 0.000002	5	2454960.3876333 ± 0.0001131	7.834436247 ± 0.000001137
Kepler-411d	2454984.8484 ± 0.0061	58.02035 ± 0.00056	5	2454984.8478013 ± 0.0005473	58.02023116 ± 0.00004203
Kepler-412b	2454966.02102000 ± 0.00002357	1.7208612825 ± 0.0000000491	2	2454966.02101665 ± 0.00002771	1.72086125797 ± 0.00000005710
Kepler-448b	2454979.59635000 ± 0.00002880	17.8552258437 ± 0.0000006438	2	2454961.74166158 ± 0.00002718	17.8552273080 ± 0.0000005863
Kepler-538b	2455044.6789 ± 0.0010	81.73778 ± 0.00013	6	2454962.9402449 ± 0.0007438	81.73797957 ± 0.00007330
Kepler-1517b	2454966.50342000 ± 0.00006786	5.5460843094 ± 0.0000004568	2	2454955.4112371 ± 0.0000758	5.5460845139 ± 0.0000005019
		Planet candidates			
Candidate name	Archival T_0 (BJD)	Archival period (d)		Updated T_0 (BJD)	Updated period (d)
K00005.01	2454965.974086 ± 0.000148	4.780327581 ± 0.000000852		2454956.4131442 ± 0.0003056	4.7803297849 ± 0.0000006835
K00075.01	2454989.97935 ± 0.00101	105.8817667 ± 0.0001312		2454989.9831552 ± 0.0003309	105.88145696 ± 0.00004402
K00076.01	2454987.70734 ± 0.00230	77.4794704 ± 0.0002456		2454987.7051992 ± 0.0001855	77.47983018 ± 0.00001939
K06068.01	2454967.4228253 ± 0.0000879	6.15025138 ± 0.00000070		2454955.12232977 ± 0.00003749	6.1502525063 ± 0.0000003761

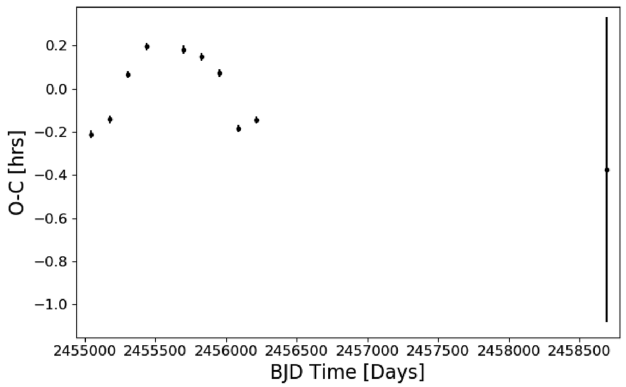

Figure 5. O–C plot for Kepler-51d, showing evidence of transit timing variations after a linear ephemeris fit.

data (due to the relatively long 58 d period), this occurred over 3 h before the expected epoch based on ephemerides in literature. Previous to this new *TESS* data, Kepler-411d had transit timing variations not explained by the inner planets in the system (Kepler-411b & c), with amplitudes of approximately 1 h. Sun et al. (2019) analysed these same TTVs (see fig. 8 from Sun et al. 2019) and found that they were best modelled by considering an extra non-transiting planet (31.5 d period) in the Kepler-411 system, Kepler-411e. However, the new *TESS* data suggests that the TTV amplitude may be much larger than previously thought, so more data (both photometric and spectroscopic) is recommended in order to constrain the parameters of this planetary system. Similarly large amplitude O–C variations were seen for Kepler-396c, so it is imperative that transit timing variations are taken into account when forecasting future observations in the Kepler-396 system (Fig. 11).

Other than those systems discussed above, the confirmed planetary systems which received updated linear ephemerides in this work had transits that aligned well with the previous *Kepler* observations and thus should be trustworthy for future observations. However, some care should be taken when forecasting individual transits within these systems, as approximately half of the updated systems exhibited non-linear behaviour in their O–C diagrams.

4.2 Planet candidates

While issues such as transit epochs falling outside the *TESS* observation window and the increased scatter of *TESS* data precluded updating the ephemerides for the majority of the 28 *Kepler* candidates, the *TESS* data provided sufficient sensitivity to update four systems: KOI-5, KOI-75, KOI-76, and KOI-6068. The new ephemerides for the candidates in these systems can be found in the second part of Table 2. The inclusion of the *TESS* data significantly decreased the uncertainty in both the initial transit time (T_0) and the period for these candidates. This new data was most helpful for the two longer period candidates, K00075.01 (105.9 d period) and K00076.01 (77.5 d period), reducing their uncertainties by almost an order of magnitude despite only single transits being present in the comparatively short-duration *TESS* observations. Care must be taken when using these new linear ephemerides however, as some evidence of transit timing variations can be seen in the O–C diagrams for both candidates (K00075.01 – Fig. 8; K00076.01 – Fig. 9).

In the case of K00075.01, the O–C plot resulting from the weighted linear fit is clearly not linear, suggesting that it would be better fit with a non-linear ephemeris. Van Eylen et al. (2019) previously fit a

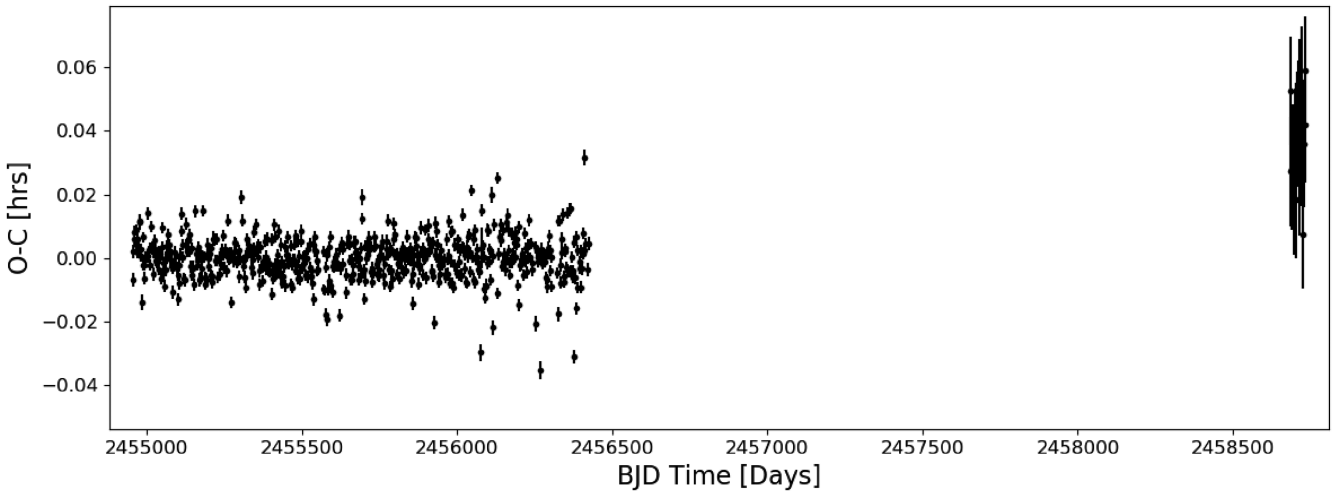

Figure 6. O–C plot for HAT-P-7b, showing notable offset between *Kepler* (BJD < 24565000) and *TESS* (BJD > 2458500) data sets.

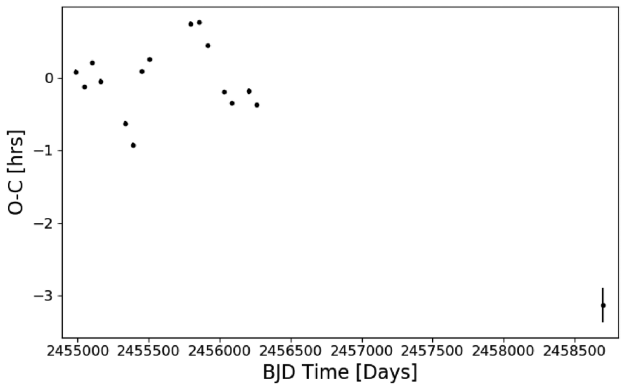

Figure 7. O–C plot for Kepler-411d, illustrating the 3 d shift between the Kepler data and single *TESS* data point.

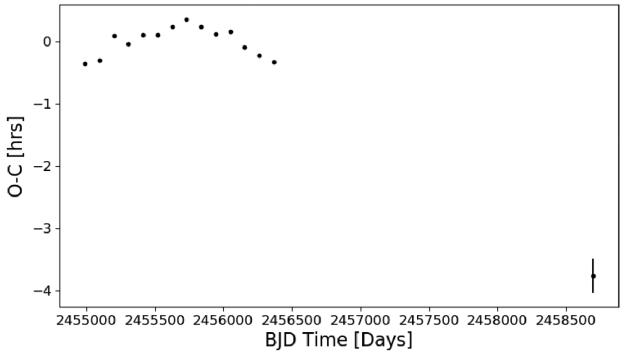

Figure 8. O–C plot for *Kepler* candidate K00075.01 after fitting the linear ephemeris derived in this work. A non-linear ephemeris is considered more appropriate for this object, however is left for the future when more *TESS* datapoints are available.

sinusoidal model to the O–C plot for K00075.01, which suggested a period of 1892 d and a TTV amplitude of 22 min. However, the new *TESS* data point suggests a considerably larger amplitude is more appropriate. It is hoped that further transits of this candidate system from the extended *TESS* mission will help to constrain the long-term TTV behaviour further.

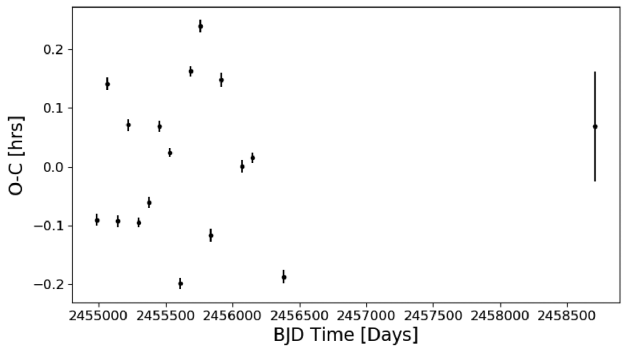

Figure 9. O–C plot for *Kepler* candidate K00076.01. Some evidence of short-term transit-timing variations are apparent.

Meanwhile, although the long-term trend of the K00076.01 system's ephemeris appears linear, there is evidence of shorter term transit timing variations, with an amplitude of approximately 0.2 h. This may be partially due to the stellar variability clear in the *Kepler* light curve, which has peak and trough-like features on a similar time-scale to the transit duration. Perhaps because of this variability, K00076.01 has been variously labelled both a candidate and false positive by different *Kepler* KOI data releases, though most recently a candidate. More in-depth analysis of this individual system is recommended in future to test its planetary nature.

It should also be noted that while the O–C diagram for K06068.01 is flat and well-constrained, it has been labelled as a false positive in some past catalogues (e.g. q1_q16_koi, Mullally et al. 2015; q1_q17_dr25_koi, Thompson et al. 2018). None the less, since the *TESS* transit appears planet-like and the system was considered a candidate in the most recent cumulative and q1_q17_dr25_sup_koi KOI deliveries, it is still retained here. In contrast, candidate transits were also plausibly recovered for K00971.01, however eyeballing of this object in the higher cadence *TESS* data suggested that host star variability is a more likely hypothesis (see Fig. 10).

Thus while follow-up of *Kepler* candidates with data from *TESS* is somewhat hampered by the short observation windows and decreased sensitivity, this new source of data provides significant opportunities for improved characterization of *Kepler* candidates, both in transit timing and shape. This is particularly true for long-period *Kepler*

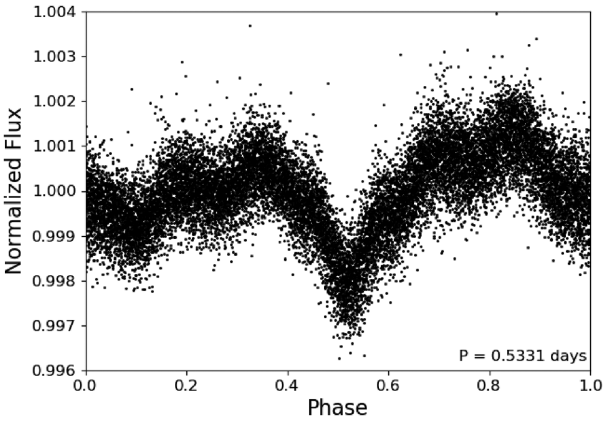

Figure 10. *Kepler* candidate K00971.01 phase folded by KOI period. The faster cadence *TESS* 2 min data reveals significant evidence of stellar activity instead of a true planetary signal.

candidates, where relatively few data points exist in the *Kepler* data alone. Furthermore, the shorter cadence *TESS* data are already revealing further details in the photometry to help to separate true planets/candidates from alternate false-positive scenarios.

4.3 TTV analysis

TTV fits were attempted for *Kepler* multiplanet systems known to exhibit significant TTVs that were re-observed by *TESS*. Five systems we identified had at least one planet with ephemerides recoverable from *TESS* data: Kepler-18, Kepler-25, Kepler-51, Kepler-89, and Kepler-396. Inferred masses for the planets in these systems are shown in Table 3, giving the median and 68.3 per cent credible region of the MCMC posteriors for both default and high mass runs. Fig. 11 demonstrates the TTV results for the two-planet Kepler-396 system using the default prior as an example.

While continued transit timing variations were clear in most systems, any differences between the mass results before and after the *TESS* datapoints are well within error, and uncertainties on masses did not consistently decrease with the additional data. We conclude that the TTV fits did not improve with the *TESS* datapoints, which we attribute to the large uncertainties associated with each new transit time, which were often larger than the TTV amplitudes themselves. Overall, the analysis is challenged by the faintness of the *Kepler* targets, and the difficulty to see individual transits in the *TESS* data.

5 DISCUSSION

Precise and accurate ephemerides are crucial to the success and efficiency of future planet characterization missions such as *JWST*. Without regular updates to their ephemerides, increasing timing uncertainties in known planets and planet candidates lead to increased observation costs and lost time, especially for longer period systems.

In this work, the ephemerides of 22 *Kepler* planets and 4 planet candidates have been updated by analysing new transits in the 2 min-cadence data from *TESS*'s primary mission. However, the extent to which ephemeris updates were possible was less than was originally anticipated. The analysis carried out by Christ et al. (2018) prior to the observations of the *Kepler* field by *TESS* was found to be excellent for determining recovery, however was perhaps a little optimistic for individual transit fitting. This was particularly the case for targets such as Kepler-10b, Kepler-93b, Kepler-138c, and Kepler-411b (Batalha et al. 2011; Kipping et al. 2014; Marcy et al. 2014;

Table 3. Overview of all TTV masses inferred in this work. Central values are the median of the MCMC posteriors, while lower and upper uncertainties are calculated from the 15.9th and 84.1th percentiles, representing the 68.3 per cent credible region.

Default prior			
Planet name	Period (d)	Mass ($M_\oplus$) (*Kepler*)	Mass ($M_\oplus$) (*Kepler* + *TESS*)
Kepler-18c	7.64	$8.6^{+5.4}_{-3.5}$	$8.4^{+5.6}_{-3.3}$
Kepler-18d	14.86	$8.5^{+2.5}_{-2.5}$	$8.4^{+2.6}_{-2.3}$
Kepler-25b	6.24	$1.0^{+1.1}_{-0.5}$	$1.2^{+1.5}_{-0.5}$
Kepler-25c	12.72	$4.5^{+3.2}_{-1.9}$	$5.0^{+3.7}_{-1.9}$
Kepler-51b	45.16	$0.9^{+1.3}_{-0.8}$	$1.1^{+1.2}_{-0.9}$
Kepler-51c	85.32	$2.8^{+0.5}_{-0.4}$	$2.8^{+0.5}_{-0.4}$
Kepler-51d	130.18	$4.4^{+1.1}_{-0.9}$	$4.4^{+1.0}_{-0.9}$
Kepler-89c	10.42	$5.3^{+2.0}_{-1.5}$	$5.2^{+2.1}_{-1.5}$
Kepler-89d	22.34	$39.4^{+9.0}_{-8.1}$	$39.3^{+8.9}_{-9.0}$
Kepler-396b	42.99	$1.4^{+0.1}_{-0.1}$	$1.4^{+0.1}_{-0.1}$
Kepler-396c	88.51	$1.1^{+0.1}_{-0.1}$	$1.1^{+0.1}_{-0.1}$
Highmass prior			
Planet name	Period (d)	Mass ($M_\oplus$) (*Kepler*)	Mass ($M_\oplus$) (*Kepler* + *TESS*)
Kepler-18c	7.64	$14.9^{+3.8}_{-3.9}$	$15.1^{+3.8}_{-3.7}$
Kepler-18d	14.86	$11.3^{+1.3}_{-1.6}$	$11.4^{+1.3}_{-1.5}$
Kepler-25b	6.24	$4.8^{+3.8}_{-2.2}$	$5.0^{+3.9}_{-2.2}$
Kepler-25c	12.72	$11.7^{+2.8}_{-3.2}$	$11.9^{+2.7}_{-3.0}$
Kepler-51b	45.16	$2.2^{+1.3}_{-1.1}$	$2.3^{+1.3}_{-1.1}$
Kepler-51c	85.32	$3.3^{+0.4}_{-0.4}$	$3.4^{+0.4}_{-0.4}$
Kepler-51d	130.18	$5.2^{+1.0}_{-1.0}$	$5.2^{+1.0}_{-1.0}$
Kepler-89c	10.42	$7.6^{+2.5}_{-1.9}$	$7.5^{+2.4}_{-1.9}$
Kepler-89d	22.34	$42.6^{+7.7}_{-7.3}$	$42.1^{+7.8}_{-7.4}$
Kepler-396b	42.99	$1.4^{+0.1}_{-0.1}$	$1.4^{+0.2}_{-0.1}$
Kepler-396c	88.51	$1.1^{+0.1}_{-0.1}$	$1.2^{+0.2}_{-0.1}$

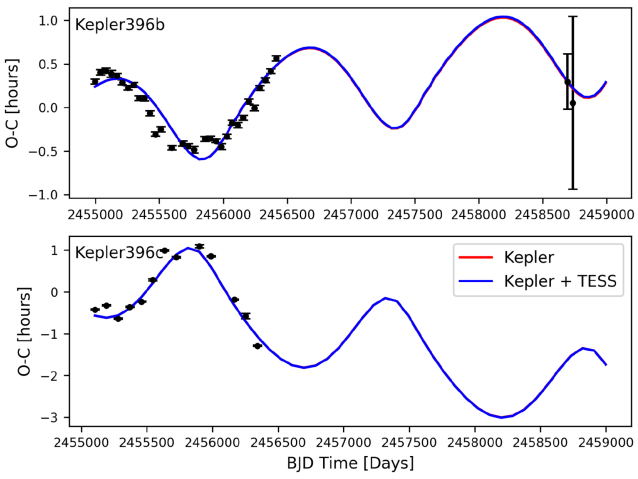

Figure 11. O–C diagrams for the Kepler-396 system (b: top; c: bottom) showing clear evidence of transit timing variations for each planet. The best-fitting TTV results assuming a default prior, using only *Kepler* data (red) and using the additional *TESS* data for Kepler-396b (blue), are plotted. The solutions lie almost directly on top of one another.

Wang et al. 2014), which were recovered when all transits were considered, but too shallow to allow individual transits to be fit reliably. For these objects (and other objects of similarly low signal to noise), an alternative method of ephemeris update is advised, perhaps by averaging all *TESS* observations by sector/year.

On a similar note, the null-result of the updated TTV analysis is an important, yet slightly disheartening one, as it suggests that updating inferred planet masses from TTVs with *TESS* may be more challenging than the community hoped. Both the Kepler-396 and Kepler-51 systems were highlighted as high priority systems for improvement with *TESS* by Goldberg et al. (2018), yet neither was significantly improved by the data from the *TESS* primary mission. The biggest challenge faced in updating these TTV masses is the faintness of most *Kepler* systems with significant transit timing variations in the *TESS* photometry, leading to very large uncertainties in individual transit times. When coupled with the fact that the systems analysed typically only had 1–3 transits in the *TESS* data, the new data is not yet very constraining. It is hoped that this situation will improve as the *TESS* extended mission continues.

These results provide an interesting comparison of *Kepler* and *TESS* photometry in practice and illustrate the differences between optimization of *TESS* and *Kepler* instruments. One thing that is immediately clear is how impressive the *Kepler* satellite was for analysis of ephemerides and TTVs for fainter stars. These differences are particularly striking in Fig. 2, clearly illustrating the difference in noise in the *Kepler* and *TESS* observations. The fact that the new *TESS* data did not significantly change the uncertainties in the periods for those analysed by Gajdos et al. (2019) is testament both to their analysis and the very high quality of *Kepler data*. For short-period *Kepler* planets with many transits in the *Kepler* data, it is perhaps unsurprising that only 1–3 sectors of *TESS* data would change the already very precise ephemerides. This is especially the case for such dim stars as make up the bulk of the *Kepler* field, since *TESS* is deliberately designed to search for planets around brighter stars (Ricker et al. 2014). None the less, for those planets without Gajdos et al. (2019) ephemerides, *TESS* has once again proven itself a very powerful tool for improving the precision of planet and candidate ephemerides, decreasing period uncertainty by orders of magnitude in cases such as HAT-P-7/Kepler-2b, Kepler-411d, Kepler-538b, and the candidates K00075.01/K00076.01.

One limitation of this work is that it focused only on *Kepler* targets which received 2 min data from the *TESS* mission. While this data set represents the shortest cadence data so far released by the *TESS* mission, it suffers from the choices made for which systems were put forward for 2 min data collection. Given that the *TESS* 2 min catalogue prioritizes bright dwarf stars in its search for smaller planets (Stassun et al. 2019), many of the dim stars in the *Kepler* field did not receive 2 min data. The analysis completed by Christ et al. (2018) demonstrates the significant promise of extending this analysis to the *TESS* full frame images (FFIs), especially when the *Kepler* field is revisited in extended mission. Such an analysis has the potential to increase the number of updated ephemerides from the approximately 25 systems updated here to hundreds of systems. This analysis is made significantly easier with the recent release of the *TESS* SPOC (Jenkins et al. 2016; Caldwell et al. 2020) and Quick Look Pipeline (Huang et al. 2020) FFI light-curves on MAST. The planned 10 min cadence data will also help considerably with this effort.

However, given the challenges faced in this study due to the dimness of many *Kepler* planets and candidates, it is imperative that we also find alternative methods/data sources to maintain the ephemerides of dim or small *Kepler* planets/candidates. Failing to do so risks letting many interesting systems fade into timing uncertainty oblivion.

6 SUMMARY

In this work, ephemerides have been updated for 22 *Kepler* planets and 4 planet candidates using short-cadence data from the *Transiting Exoplanet Survey Satellite*. This represents all *Kepler* planets and candidates which so far have received *TESS* 2 min data with sufficient signal to noise to allow ephemeris updates to be carried out. The primary challenges to updating more systems were long period planets/candidates falling outside the *TESS* observation window, and systems being too dim in the *TESS* data. Because of the dimness of these objects, a purely photometric method was used to updated these ephemerides, using transits from *Kepler* and *TESS* data only. Transit times for individual transits were recovered by using an MCMC fit of a transit model based on stacked *Kepler* transits. These transit times were then fit a weighted-linear fit in order to obtain the final ephemerides for each object. Any systems which did not appear to have significant transit timing variations were additionally fit with a simultaneous *TESS/Kepler* fit to improve the epehmerides further. The resulting ephemerides were in good agreement with archival ephemerides and drastically reduced the uncertainty in period for Kepler-411d, Kepler-538b, and the candidates K00075.01/K00076.01. Residuals to the linear ephemeris fits gave an important window into transit timing variations for these objects. TTV fits were attempted for five multiplanet systems known to exhibit significant TTVs (Kepler-18, Kepler-25, Kepler-51, Kepler-89, and Kepler-396), however these were challenged by the relative scarcity of reasonable *TESS* transits and the dimness of these systems in *TESS*. In the end there were no significant differences between the TTV masses before and after the inclusion of the *TESS* data. More data are required (preferably of higher signal to noise) in order to constrain the TTV masses more effectively. Interesting TTV behaviour was observed also in the O–C diagrams for HAT-P-7b/Kepler-2b, Kepler-411d, K00075.01, and K00076.01, which warrants further analysis when new data becomes available. Thus while ephemeris updates and TTV analysis of *Kepler* systems reobserved by *TESS* proved less constraining than originally anticipated, *TESS* has once again proved itself as an important follow-up instrument in addition to its primary planet-finding and asteroseismic aims. Overall, the ephemerides improved and updated in this study extend the life of these *Kepler* systems, and improve prospects for future characterization. Significant additional benefits are likely if the methods outlined in this paper are extended to the much larger sample of planets and candidates reobserved in the *TESS* 30 min cadence data, especially as *TESS* returns to the *Kepler* field in its extended mission. Care must be taken however to ensure that the community develops equipment and methods to maintain the ephemerides of dimmer *Kepler* systems, as many of these are simply too dim to be followed up by *TESS*.

ACKNOWLEDGEMENTS

The authors would like to thank the anonymous referee for their comments which improved the quality and robustness of this paper. MPB wishes to acknowledge A Osborn for their helpful `exoplanet` tutorial.

This research made use of `exoplanet` (Foreman-Mackey et al. 2020) and its dependencies (Astropy Collaboration 2013, 2018; Kipping 2013; Salvatier et al. 2016; Theano Development Team

2016; Kumar et al. 2019; Agol, Luger & Foreman-Mackey 2020; Foreman-Mackey et al. 2020). This paper includes data collected by the Kepler mission. Funding for the Kepler mission is provided by the NASA Science Mission Directorate. This paper includes data collected by the *TESS* mission. We acknowledge the use of public TOI Release data from pipelines at the *TESS* Science Office and at the *TESS* Science Processing Operations Center. Funding for the *TESS* mission is provided by NASA's Science Mission directorate. This research has made use of the Exoplanet Follow-up Observation Program website, which is operated by the California Institute of Technology, under contract with the National Aeronautics and Space Administration under the Exoplanet Exploration Program. *TESS* and *Kepler* data were obtained from the Mikulski Archive for Space Telescopes (MAST). STScI is operated by the Association of Universities for Research in Astronomy, Inc., under NASA contract NAS5-26555. Support for MAST is provided by the NASA Office of Space Science via grant NNX13AC07G and by other grants and contracts.

This research has made use of the NASA Exoplanet Archive, which is operated by the California Institute of Technology, under contract with the National Aeronautics and Space Administration under the Exoplanet Exploration Program.

MPB acknowledges support from the University of Warwick via the Chancellor's International Scholarship. DJA acknowledges support from the STFC via an Ernest Rutherford Fellowship (ST/R00384X/1).

DATA AVAILABILITY

The new ephemeris data generated in this article are available in the article and in its online supplementary material. The derived O–C transit timing data for individual planets analysed in this work will be shared on reasonable request to the corresponding author. All planet and candidate light curves analysed in this work were drawn from public *TESS* and *Kepler* data hosted on the Mikulski Archive for Space Telescopes (MAST) Portal.[8] Additional parameters for the planet and candidate systems were drawn from the Exoplanet Archive,[9] as discussed in the main text.

REFERENCES

Agol E., Luger R., Foreman-Mackey D., 2020, AJ, 159, 123
Astropy Collaboration, 2013, A&A, 558, A33
Astropy Collaboration, 2018, ApJ, 156, 123
Batalha N. M. et al., 2011, ApJ, 729, 27
Battley M. P., Pollacco D., Armstrong D. J., 2020, MNRAS, 496, 1197
Berger T. A., Huber D., Gaidos E., van Saders J. L., 2018, ApJ, 866, 99
Bonomo A. S. et al., 2017, A&A, 602, A107
Borucki W. J. et al., 2010, Science, 327, 977
Borucki W. J. et al., 2011, ApJ, 736, 19
Bourrier V. et al., 2015, A&A, 579, A55
Buchhave L. A. et al., 2011, ApJS, 197, 3
Caldwell D. A. et al., 2020, Res. Notes Am. Astron. Soc., 4, 201
Christ C. N., Montet B. T., Fabrycky D. C., 2018, AJ, 157, 235
Cleveland W. S., 1979, J. Am. Stat. Assoc., 74, 829
Cochran W. D. et al., 2011, ApJS, 197, 7
Deck K., Agol E., Holman M., Nesvorny D., 2014, Astrophysics Source Code Library, record ascl:1404.015
Deleuil M. et al., 2014, A&A, 564, A56
Dragomir D. et al., 2020, AJ, 159
Edwards B. et al., 2020, MNRAS, in press
Foreman-Mackey D. et al., , 2020, exoplanet-dev/exoplanet v0.4.3
Foreman-Mackey D., Hogg D. W., Lang D., Goodman J., 2012, PASP, 125, 306
Fressin F. et al., 2011, ApJS, 197, 5
Gaia Collaboration Brown A. G. A., Vallenari A., Prusti T., de Bruijne J. H. J., Babusiaux C., Bailer-Jones C. A. L., 2018, A&A, 616, 22
Gajdoš P., Parimucha S., Hambálek L., Vanko M., 2017, MNRAS, 469, L2907
Gajdos P., Vanko M., Parimucha S., 2019, Res. in Astron. and Astrophys., 19, 41
Gardner J. P. et al., 2006, Space Sci. Rev., 123, 485
Gilliland R. L. et al., 2011, ApJS, 197 , 6
Gilliland R. L. et al., 2013, ApJ, 766, 40
Goldberg M., Hadden S., Payne M. J., Holman M. J., 2018, AJ, 157, 152
Szabó, G. et al., 2020, MNRAS, 492, L17
Hadden S., Lithwick Y., 2016, ApJ, 828, 44
Hadden S., Lithwick Y., 2017, AJ, 154, 5
Hartman J. D., Bakos G., 2016, Astron. Comput., 17, 1
Holczer T. et al., 2016, ApJS, 225, 9
Holman M. J. et al., 2010, Science, 330, 51
Howell S. B. et al., 2012, ApJ, 746, 123
Howell S. B. et al., 2014, PASP, 126, 938
Huang C. X. et al., 2020, Res. Notes Am. Astron. Soc., 4, 206
Ikwut-Ukwa M. et al., 2020, Am. Astron. Soc J., 160, 209
Jenkins J. M. et al., 2010, ApJ, 713 , L87
Jenkins J. M. et al., 2016, in Chiozzi G., Guzman J. C., eds, Proc. SPIE Conf. Ser. Vol. 9913, Software and Cyberinfrastructure for Astronomy IV. SPIE, Bellingham, p. 99133E
Jontof-Hutter D., Wolfgang A., Ford E. B., Lissauer J. J., Fabrycky D. C., Rowe J. F., 2021, preprint (arXiv:2101.01202)
Kipping D., Nesvory D., Buchhave L., Hartman J., Bakos G. A., Schmitt A., 2014, ApJ, 784, 28
Kipping D. M., 2013, MNRAS, 435, 2152
Kokori A. et al., 2020, preprint(arxiv:2012.07478)
Kovács G., Zucker S., Mazeh T., 2002, A&A, 391 , 369
Kreidberg L., 2015, PASP, 127, 1161
Kumar R., Carroll C., Hartikainen A., Martin O. A., 2019, J. Open Source Softw., 4, 1143
Lightkurve Collaboration, 2018, Astrophysics Source Code Library, record ascl:1812.013
Lindegren L. et al., 2018, A&A, 616, A2
Livingston J. H. et al., 2019, AJ, 157, 102
Mandel K., Agol E., 2002, ApJ, 580, L171
Marcy G. W. et al., 2014, ApJS, 210, 20
Martin D. V., 2017, MNRAS, 465, 3235
Masuda K., 2014, ApJ, 783, 53
Mayo A. W. et al., 2019, AJ, 158, 165
Morton T. D., Bryson S. T., Coughlin J. L., Rowe J. F., Ravichandran G., Petigura E. A., Haas M. R., Batalha N. M., 2016, ApJ, 822, 86
Mullally F. et al., 2015, ApJS, 217, 31
Pál A. et al., 2008, ApJ, 680, 1450
Poddaný S., Brát L., Pejcha O., 2010, New Astron., 15, 297
RickerG. et al., 2014, J. of Astron. Telesc., Instrum and Syst., 1, 014003
Rowe J. F. et al., 2014, ApJ, 784, 45
Salvatier J., Wiecki T. V., Fonnesbeck C., 2016, PeerJ Comput. Sci., 2, e55
Sanchis-Ojeda R. et al., 2013, ApJ, 775, 54
Stassun K. G. et al., 2019, AJ, 158, 138
Steffen J. H. et al., 2012, MNRAS, 421, 2342
Steffen J. H. et al., 2013, MNRAS, 428, 1077
Sun L., Ioannidis P., Gu S., Schmitt J. H. M. M., Wang X., Kouwenhoven M. B. N., 2019, A&A, 624, A15
Su K. Y. L., Rieke G. H., Melis C., Jackson A. P., Smith P. S., Meng H. Y. A., Gaspar A., 2020, ApJ, 898, 21
Theano Development Teamet al., 2016, preprint(arXiv: 1605.02688)
Thompson S. E. et al., 2018, ApJS, 235, 38
Thompson S. E., Fraquelli D., Van Cleve J. E., Caldwell D. A., 2016, Technical report, Kepler Archive Manual. NASA
Van Eylen V. et al., 2019, ApJ, 157, 61

[8] https://mast.stsci.edu/portal/Mashup/Clients/Mast/Portal.html
[9] https://exoplanetarchive.ipac.caltech.edu/

Wang J., Xie J.-W., Barclay T., Fischer D. A., 2014, ApJ, 783, 4
Weiss L. M. et al., 2013, ApJ, 768, 14
Welsh W. F. et al., 2015, ApJ, 809, 26
Xie J.-W., 2014, ApJS, 210, 25
Zellem R. T. et al., 2020, PASP, 132, 054401

SUPPORTING INFORMATION

Supplementary data are available at *MNRAS* online.

Please note: Oxford University Press is not responsible for the content or functionality of any supporting materials supplied by the authors. Any queries (other than missing material) should be directed to the corresponding author for the article.

APPENDIX A: OVERVIEW OF ALL *KEPLER* SYSTEMS WITH *TESS* 2MIN DATA

Table A1 summarizes all *Kepler* systems with known transiting planets which received short-cadence (2 min) data in *TESS*'s Primary Mission. For each system all known planets are listed, along with whether their ephemerides were updated. For planets which were theoretically reobserved but not updated in this work, a brief explanation is supplied for their exclusion. Most commonly this is because their expected transits fell outside the eventual *TESS* observation window, or they were shallow enough that any potential transits were lost in the increased noise of the *TESS* data.

Table A1. Overview of all *Kepler* planetary systems which received *TESS* short cadence data during *TESS*'s Primary Mission. N.b. 'outside' = any planets whose expected transit epochs fell outside times of *TESS* observations; 'shallow' = planets with transits which were sufficiently shallow for individual transits to be indiscernible from noise in the *TESS* data.

Kepler name	TIC ID	Ephemeris updated?	Reason for exclusion
Kepler-2b	TIC 424865156	**Yes**	–
Kepler-9b,c,d	TIC 120571842	No	c outside; b,d shallow
Kepler-10b,c	TIC 377780790	**Yes** - c, No - b	b shallow
Kepler-11b,c,d,e,f,g	TIC 169175503	No	All shallow
Kepler-13b	TIC 158324245	**Yes**	–
Kepler-14b	TIC 158561566	**Yes**	–
Kepler-16b	TIC 299096355	No	Outside
Kepler-18b,c,d	TIC 273690178	**Yes** - d, No b,c	b,c shallow
Kepler-21b	TIC 121214185	No	Shallow
Kepler-25b,c,d	TIC 120960812	**Yes** - b,c; No - d	d outside
Kepler-30b,c,d	TIC 399794329	No	b shallow; c,d outside
Kepler-34b	TIC 272369124	No	Outside
Kepler-35b	TIC 271040768	No	Outside
Kepler-36b,c	TIC 350810590	No	Shallow
Kepler-38b	TIC 158316612	No	Outside
Kepler-47b,c,d	TIC 271548206	No	b shallow; c,d outside
Kepler-51b,c,d	TIC 27846348	**Yes** - b,d; No - c	c shallow
Kepler-63b	TIC 299158887	**Yes**	–
Kepler-65b,c,d,e	TIC 121731834	No	b,c,d shallow; e outside
Kepler-68 b,c	TIC 417676622	**Yes** -b; No c	c shallow
Kepler-78b	TIC 270701667	No	Shallow
Kepler-79b,c,d,e	TIC 239306681	No	All shallow
Kepler-83b,c,d	TIC 123416515	No	All shallow
Kepler-89b,c,d,e	TIC 273231214	**Yes** - d; No - b,c,e	b,c shallow; e outside
Kepler-91b	TIC 352011875	No	Shallow
Kepler-93b,c	TIC 137151335	No	b shallow; c outside
Kepler-96b	TIC 169081296	**Yes**	–
Kepler-122b,c,d,e	TIC 122714267	No	b,c,d shallow; e outside
Kepler-138b,c,d	TIC 159376971	No	b,c shallow; d outside
Kepler-289b,c,d	TIC 273234825	**Yes** - d; No - b,c	b shallow; c outside
Kepler-297b,c	TIC 48304302	No	Both shallow
Kepler-381b,c	TIC 164884235	No	Both shallow
Kepler-396b,c	TIC 27769688	**Yes**	–
Kepler-408b	TIC 48450369	No	Shallow
Kepler-409b	TIC 270619260	No	Shallow
Kepler-411b,c,d	TIC 399954349	**Yes** - c,d; No b	b shallow
Kepler-412b	TIC 158170594	**Yes**	–
Kepler-413b	TIC 298969838	No	Outside
Kepler-448b,c	TIC 169461816	**Yes** - b; No - c	c outside
Kepler-453b	TIC 164457525	No	No longer transiting
Kepler-462b	TIC 269263577	No	Shallow
Kepler-508b	TIC 271671025	No	Shallow
Kepler-538b	TIC 28227113	**Yes**	–
Kepler-1084b	TIC 267749737	No	Shallow
Kepler-1244b	TIC 123447592	No	Shallow
Kepler-1517b	TIC 158555987	**Yes**	–
Kepler-1647b	TIC 170344769	No	Outside
Kepler-1661b	TIC 164886585	No	Outside
PH1 b	TIC 170348142	No	Outside

This paper has been typeset from a TEX/LATEX file prepared by the author.